Reversible Olefin−Hydride Insertion in the Cationic Ruthenium Complexes $[(\eta^6\text{-}C_6H_5CH_2CH_2PR_2)RuH(CH_2{=}CH_2)]^+$

Kayo Umezawa-Vizzini and T. Randall Lee*

Department of Chemistry, University of Houston, 4800 Calhoun Road, Houston, Texas 77204-5003

Received March 14, 2003

Ruthenium−hydride olefin complexes having the formula $[(\eta^6\text{-}C_6H_5CH_2CH_2PR_2)RuH(CH_2{=}CH_2)][PF_6]$, where R = Cy (**1**) and Ph (**2**), were prepared via the reaction of triphenylcarbenium hexafluorophosphate (Ph_3CPF_6) with the corresponding $(\eta^6\text{-}C_6H_5CH_2CH_2PR_2)Ru(CH_3)_2$ complexes. Reversible olefin−hydride insertion reactions were directly observed for both **1** and **2** by 2D EXSY magnetic resonance experiments. The structure of complex **1** was determined by X-ray crystallography.

Introduction

The insertion of carbon−carbon double bonds into metal−hydride bonds occurs during many transition metal-catalyzed transformations of olefins (e.g., olefin hydrogenation, hydroformylation, and isomerization).[1] From a fundamental point of view, the insertion of an olefin into a metal−hydride bond is analogous to the insertion of an olefin into a metal−alkyl bond, which represents perhaps the most critical step in the catalytic polymerization of olefins.[2] Since the energy barrier for olefin insertion into metal−hydride bonds is lower than that for insertion into metal−alkyl bonds,[3,4] relatively few metal−hydride olefin complexes have been reported in the literature; in contrast, metal−alkyl olefin complexes are abundant.[5,6]

Of the known metal−hydride olefin complexes, most exhibit reversible olefin−hydride insertion. For example, reversible insertion has been directly observed in a variety of organometallic complexes centered with transition metals such as Mo,[7] Co,[3,4,8] Rh,[3,4,9] Pt,[10] Ru,[11,12] Nb,[13] and Ta[14] using variable-temperature nuclear magnetic resonance (NMR) spectroscopy, dynamic NMR spectroscopy, and magnetization-transfer studies. For ruthenium, however, examples of reversible olefin−hydride insertion are extremely rare. Faller, for example, observed the reversible insertion of styrene into the Ru−hydride bond of the minor diastereomer of $[(p\text{-cymene})RuH(CH_2{=}CHPh)PR_3][SbF_6]$ (R = Ph, OMe) by magnetization transfer.[11] Furthermore, Yi and Lee found evidence of ethylene insertion into the Ru−H of $(PCy_3)_2(CO)(Cl)RuH$ upon treatment of the complex with ^{13}C-labeled ethylene.[12] In general, however, mononuclear Ru−hydride olefin complexes are stable and exhibit characteristically well-separated hydride chemical shifts by ^1H NMR spectroscopy, which is consistent with the absence of reaction between the hydride and the olefin.[15−17]

Recently, much research has targeted the development of Ziegler−Natta olefin polymerization catalysts based on late transition metals such as Co,[18−21] Ni,[22−24,27−29] Pd,[22−24] and Fe.[18−21,25,26] In contrast, Ru-based Ziegler−Natta polymerization catalysts have been limited to a few example polymerizations of ethylene.[30−32] For the past few years, we have been exploring the

* To whom correspondence should be addressed. E-mail: trlee@uh.edu.

(1) See, for example: Ojima, I.; Eguchi, M.; Tzamarioudaki, M. In *Comprehensive Organometallic Chemistry*; Abel, E. W., Ed.; Pergamon: New York, 1995; p 39.
(2) Siegbahn, E. M. *J. Am. Chem. Soc.* **1993**, *115*, 5803.
(3) Schmidt. G. F.; Brookhart, M. *J. Am. Chem. Soc.* **1985**, *107*, 1444.
(4) Brookhart, M.; Lincoln, D. M. *J. Am. Chem. Soc.* **1988**, *110*, 8719.
(5) Collman, J. P.; Hegedus, L. S.; Norton, J. R.; Finke, R. G. *Principles and Applications of Organotransition Metal Chemistry*; University Science: Mill Valley, CA, 1987.
(6) Flood, T. C.; Bitler, S. P. *J. Am. Chem. Soc.* **1984**, *106*, 6076.
(7) Byrne, J. W.; Blaser, H. U.; Osborn, J. A. *J. Am. Chem. Soc.* **1975**, *97*, 3871.
(8) Klein, H.-F.; Hammer, R.; Gross, J.; Schubert, U. *Angew. Chem., Int. Ed. Engl.* **1980**, *19*, 809.
(9) Brookhart, M.; Hauptman, E.; Lincoln, D. M. *J. Am. Chem. Soc.* **1992**, *114*, 10394.
(10) Chatt, J.; Coffey, R. S.; Gough, A.; Thompson, D. T. *J. Chem. Soc.* (*A*) **1968**, 190.
(11) Faller, J. W.; Chase, K. J. *Organometallics* **1995**, *14*, 1592.
(12) Yi, C. S.; Lee, D. W. *Organometallics* **1999**, *18*, 5152.
(13) Doherty, N.; Bercaw, J. E. *J. Am. Chem. Soc.* **1985**, *107*, 2670.
(14) Burger, B. J.; Santarsiero, B. D.; Trimmer, M. S.; Bercaw, J. E. *J. Am. Chem. Soc.* **1988**, *110*, 3134.
(15) Kletzin, H.; Werner, H.; Serhadli, O.; Ziegler, M. L. *Angew. Chem., Int. Ed. Engl.* **1983**, *22*, 46.
(16) Linder, E.; Pautz, S.; Fawzi, R.; Steimann, M. *Organometallics* **1998**, *17*, 3006.
(17) Werner, H.; Kletzin, H.; Hohn, A.; Paul, W.; Knaup, W.; Ziegler, M. L.; Serhadli, O. *J. Organomet. Chem.* **1986**, *306*, 227.
(18) Small, B. L.; Brookhart, M.; Bennett, A. M. *J. Am. Chem. Soc.* **1998**, *120*, 4049.
(19) Britovsek, G. J. P.; Gibson, V. C.; Kimberley, B. S.; Maddox, P. J.; McTavish, S. J.; Solan, G. A.; White, A. J. P.; Williams, D. J. *Chem. Commun.* **1998**, 849.
(20) Small, B. L.; Brookhart, M. *Polym. Prepr.* **1998**, *39*, 213.
(21) Britovsek, G. J. P.; Gibson, V. C.; Spitzmesser, S. K.; Tellmann, K. P.; White, A. J. P.; Williams, D. J. *J. Chem. Soc., Dalton Trans.* **2002**, *6*, 1159.
(22) Johnson, L. K.; Killian, C. M.; Brookhart, M. *J. Am. Chem. Soc.* **1995**, *117*, 6414.
(23) Killian, C. M.; Tempel, D. J.; Johnson, L. K.; Brookhart, M. *J. Am. Chem. Soc.* **1996**, *118*, 11664.
(24) Johnson, L. K.; Mecking, S.; Brookhart, M. *J. Am. Chem. Soc.* **1996**, *118*, 267.
(25) Brooke, L.; Brookhart, M. *Macromolecules* **1999**, *32*, 2120.
(26) Pellecchia, C.; Mazzeo, M.; Pappalardo, D. *Macromol. Rapid Commun.* **1998**, *19*, 615.
(27) Conner, E. F.; Younkin, T. R.; Henderson, J. I.; Hwang, S.; Grubbs, R. H.; Roberts, W. P.; Litzau, J. *J. Polym. Sci., Part A* **2002**, *40*, 2842.
(28) Preishuber-Pflugl, P.; Brookhart, M. *Macromolecules* **2002**, *35*, 6074.

10.1021/om0301987 CCC: $27.50
Publication on Web 01/28/2004

reaction of ruthenium alkyls with olefins in efforts to develop ruthenium-based olefin polymerization catalysts.[33−36] Ruthenium not only is isoelectronic with iron but is also known to initiate the ring-opening metathesis polymerization (ROMP) of cyclic olefins containing polar functional groups.[37−42] In this paper, we report that (η^6-$C_6H_5CH_2CH_2PR_2$)$Ru(CH_3)_2$, where R = cyclohexyl (Cy) and phenyl (Ph), affords [(η^6-C_6H_5-$CH_2CH_2PR_2$)$RuH(CH_2{=}CH_2)$][PF_6] upon reaction with triphenylcarbenium hexafluorophosphate (Ph_3CPF_6). We describe the synthesis, structural characterization, and direct observation of olefin−hydride insertion for these cationic ruthenium complexes.

Results and Discussion

Using a procedure adapted from the literature,[17] cationic ruthenium(II) complexes [(η^6-$C_6H_5CH_2CH_2PR_2$)-$RuH(CH_2{=}CH_2)$][PF_6] (**1** and **2**) were prepared by the reaction of (η^6-$C_6H_5CH_2CH_2PR_2$)$Ru(CH_3)_2$ (R = Cy and Ph, respectively) with Ph_3CPF_6 in CH_2Cl_2 (eq 1). Upon

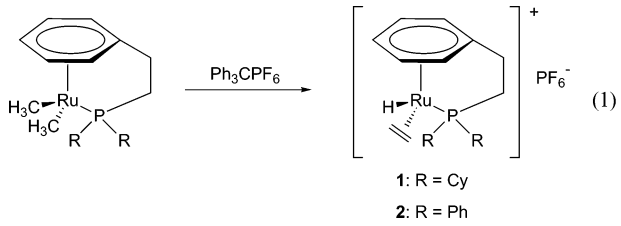

(1)

crystallization by slow evaporation of CH_2Cl_2, compound **1** was obtained as light yellow crystal that were insoluble in hexanes and diethyl ether, but slightly soluble in benzene and THF. In separate experiments, compound **2** was also isolated, but decomposed in CH_2-Cl_2 during attempted recrystallizations. For both **1** and **2**, the BF_4^- salts were prepared with similar results (data not shown).

Analogous olefin hydride complexes were obtained by Werner et al. by the reaction of (η^6-C_6H_6)$Os(CH_3)_2L$ (L = CO, PMe_3),[17,43] (η^6-C_6Me_6)$RuPR_3(CH_3)_2$ (R_3 = Ph_3, Me_3, $MePh_2$),[15−17] and $CpIr(CH_3)_2P(i\text{-}Pr)_3$[17] with Ph_3-CPF_6. The formation of **1** and **2** can be rationalized on the basis of a previously proposed mechanism analogous to that shown in eq 2.[17,43] As illustrated, the reaction

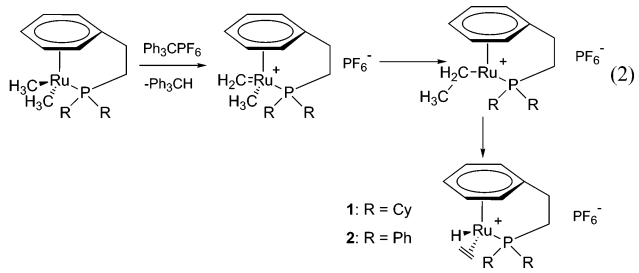

(2)

probably proceeds through the intermediacy of Ru-methylidene and Ru-ethyl species. It has not been established, however, whether the methylidene formation proceeds via radical processes such as that observed during the formation of $[Cp_2WH(CH_2{=}CH_2)]^+$ from $Cp_2W(CH_3)_2$.[44]

We performed an X-ray crystal structure analysis on a single crystal of **1** obtained from the slow evaporation of CH_2Cl_2. The resulting thermal ellipsoid plot and a view perpendicular to the η^6-aromatic ring are shown in Figure 1; selected bond distances and angles are listed in Table 1. The observed bond distance of Ru−H was 1.47 ± 0.04 Å, which is similar in magnitude to that of the related complexes [(η^6-C_6Me_6)$RuH(CH_2{=}CH_2)$-PPh_3][PF_6] (1.50 Å)[15,16] and [(*p*-cymene)$RuH(CH_2{=}$-$CHPh)PPh_3$][SbF_6] (1.44 Å).[11] The bond distance is, however, shorter than that found for other Ru−H complexes, such as $[RuH(C_{10}H_7)(dmpe)]^+$ (1.67 Å),[45] $RuHCl(PPh_3)_3$ (1.68 Å),[46] $RuH(CCPh)(P(CH_2CH_2PPh_2)_3$ (1.57 Å),[47] and [(η^6-$C_6H_5PPh_2$)$RuH(PPh_3)_2$]$^+$ (ca. 1.68 Å).[48] Although the exact determination of metal hydride positions by X-ray crystallography is not highly accurate,[5] the hydride observed here appears to reside at substantial distances, 2.25 and 2.86 Å, from the ethylene carbons, C1 and C2, respectively. Thus, we find no evidence for agostic interactions between the hydride and the olefin in the solid-state structure of **1**.[49]

The bond distances between C1 and C2 (1.37 Å) and those between the ethylenic carbons and ruthenium (Ru−C1 and Ru−C2, both 2.20 Å) are similar to those observed for [(η^6-C_6Me_6)$RuH(CH_2{=}CH_2)PPh_3$][PF_6] (1.41 Å; 2.17 and 2.19 Å, respectively)[15,16] and [(*p*-cymene)-$RuH(CH_2{=}CHPh)(PPh_3)$][SbF_6] (1.40 Å; 2.20 and 2.22 Å, respectively).[11] The equivalent Ru−C1 and Ru−C2 bond distances observed for **1** demonstrate that there is no tilting of the olefin. The three ligands exist in a staggered conformation relative to the coordinated arene. The ruthenium metal lies beneath the center of the coordinated arene. The bond distances from Ru to each carbon of the coordinated arene are 2.23 Å (Ru−C5), 2.29 Å (Ru−C6), 2.30 Å (Ru−C7), 2.32 Å (Ru−C8), 2.26 Å (Ru−C9), and 2.22 Å (Ru−C10). The slightly elongated distances for Ru−C7, Ru−C8, and Ru−C9 are probably constrained by the presence of the two-carbon bridge.

Additional characterization of the new complexes was performed using ^{1}H NMR (variable temperature), ^{13}C

(29) Liu, W.; Malinoski, J. M.; Brookhart, M. *Organometallics* **2002**, *21*, 2836.
(30) James, B. R.; Markham, L. D. *J. Catal.* **1972**, *27*, 442.
(31) Komita, S.; Yamamoto, A.; Ikeda, S. *Bull. Chem. Soc. Jpn.* **1975**, *48*, 101.
(32) Momura, K.; Warit, S.; Imanishi, Y. *Macromolecules* **1999**, *32*, 4732.
(33) Umezawa-Vizzini, K.; Lee, T. R. *Organometallics* **1997**, *16*, 5613.
(34) Umezawa-Vizzini, K.; Lee, T. R. *J. Organomet. Chem.* **1999**, *157*, 122.
(35) Umezawa-Vizzini, K.; Lee, T. R. *Organometallics* **2003**, *22*, 3059.
(36) Umezawa-Vizzini, K.; Lee, T. R. *Organometallics* **2003**, *22*, 3066.
(37) Maughon, B. R.; Grubbs, R. H. *Macromolecules* **1997**, *30*, 3459.
(38) Hillmyer, M. A.; Gutierrez, E.; Grubbs, R. H. *Macromolecules* **1995**, *28*, 7256.
(39) Hillmyer, M. A.; Laredo, W. R.; Grubbs, R. H. *Macromolecules* **1995**, *28*, 6311.
(40) Grubbs, R. H. *Macromolecules* **1997**, *30*, 3978.
(41) Lynn, D. M.; Mohr, B.; Grubbs, R. H. *J. Am. Chem. Soc.* **1998**, *120*, 1627.
(42) Maynard, H. D.; Grubbs, R. H. *Macromolecules* **1999**, *32*, 6917.
(43) Roder, K.; Werner, H. *Angew. Chem., Int. Ed. Engl.* **1987**, *26*, 686.
(44) Hayes, J. C.; Cooper, N. J. *J. Am. Chem. Soc.* **1982**, *104*, 5570.
(45) Gregory, U. A.; Ibekwe, S. D.; Kilbourn, B. T.; Russel, D. R. *J. Chem. Soc.* (*A*) **1971**, 1118.
(46) Skapski, A. C.; Troughton, P. G. H. *Chem. Commun.* **1968**, 1230.
(47) Bianchini, C.; Frediani, P.; Masi, D.; Peruzzini, M.; Zanobini, F. *Organometallics* **1994**, *13*, 4616.
(48) McConway, J. C.; Skapski, A. C.; Phillips, L.; Young, R. J.; Wilkinson, G. *Chem. Commun.* **1974**, 327.
(49) Brookhart, M.; Green, M. L. H. *J. Organomet. Chem.* **1983**, *250*, 395.

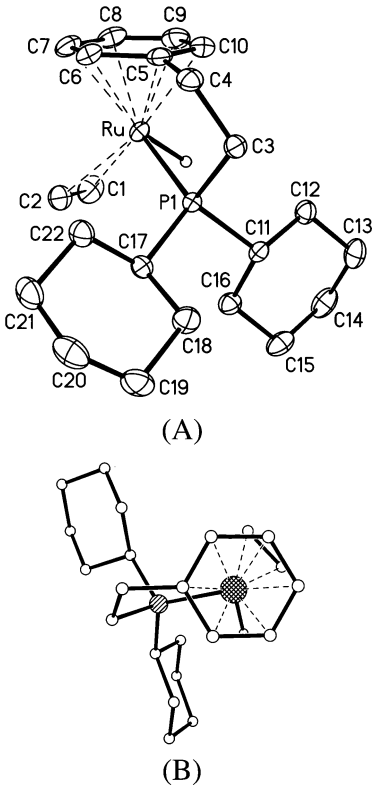

Figure 1. (A) Thermal ellipsoid plot of [(η^6-$C_6H_5CH_2CH_2PCy_2$)RuH(CH_2=CH_2)]$^+$ (**1**) at the 40% probability level and (B) a view perpendicular to the η^6-aromatic ring.

Table 1. Selected Bond Lengths [Å] and Angles [deg] for 1

	Bond Lengths		
Ru−H	1.47(4)	Ru−C(2)	2.195(4)
Ru−C(1)	2.199(4)	Ru−C(10)	2.223(3)
Ru−C(5)	2.228(3)	Ru−C(9)	2.257(3)
Ru−C(6)	2.286(3)	Ru−P(1)	2.2950(8)
Ru−C(7)	2.297(3)	Ru−C(8)	2.315(3)
C(1)−C(2)	1.367(6)		
	Bond Angles		
H−Ru−C(2)	100.8(15)	H−Ru−C(1)	72.7(15)
C(2)−Ru−C(1)	36.26(15)	H−Ru−C(10)	95.2(15)
C(2)−Ru−C(10)	164.02(14)	C(1)−Ru−C(10)	153.92(15)
H−Ru−C(5)	126.4(15)	C(2)−Ru−C(5)	128.53(14)
C(1)−Ru−C(5)	160.83(14)	C(10)−Ru−C(5)	37.27(12)
H−Ru−C(9)	87.7(15)	C(2)−Ru−C(9)	142.87(14)
C(1)−Ru−C(9)	118.07(16)	C(10)−Ru−C(9)	36.75(13)
C(5)−Ru−C(9)	66.41(13)	H−Ru−C(6)	160.8(15)
C(2)−Ru−C(6)	98.40(14)	C(1)−Ru−C(6)	124.49(14)
C(10)−Ru−C(6)	65.61(12)	C(5)−Ru−C(6)	36.49(12)
C(9)−Ru−C(6)	76.60(13)	H−Ru−P(1)	77.9(15)
C(2)−Ru−P(1)	90.71(10)	C(1)−Ru−P(1)	106.35(12)
C(10)−Ru−P(1)	93.03(9)	C(5)−Ru−P(1)	81.55(8)
C(9)−Ru−P(1)	126.40(10)	C(6)−Ru−P(1)	102.40(8)
H−Ru−C(7)	143.1(15)	C(2)−Ru−C(7)	90.05(14)
C(1)−Ru−C(7)	98.85(14)	C(10)−Ru−C(7)	76.76(13)
C(5)−Ru−C(7)	65.41(12)	C(9)−Ru−C(7)	64.17(13)
C(6)−Ru−C(7)	35.86(12)	P(1)−Ru−C(7)	137.65(9)
H−Ru−C(8)	108.3(15)	C(2)−Ru−C(8)	108.75(14)
C(1)−Ru−C(8)	96.14(15)	C(10)−Ru−C(8)	65.17(13)
C(5)−Ru−C(8)	77.46(12)	C(9)−Ru−C(8)	35.61(13)
C(6)−Ru−C(8)	64.46(12)	C(7)−Ru−C(8)	35.54(13)
P(1)−Ru−C(8)	157.47(10)	C(2)−C(1)−Ru	71.7(2)
C(1)−C(2)−Ru	72.0(2)		

NMR, ^{1}H−^{1}H COSY, and ^{1}H−^{13}C COSY spectroscopic measurements in CD_2Cl_2. At 0 °C, the ^{1}H NMR spectra of **1** and **2** exhibited broad resonances at δ −9.5 and −8.6, respectively, which can be assigned to the Ru−H moieties.[15,17,43] Variable-temperature ^{1}H NMR and ^{1}H−

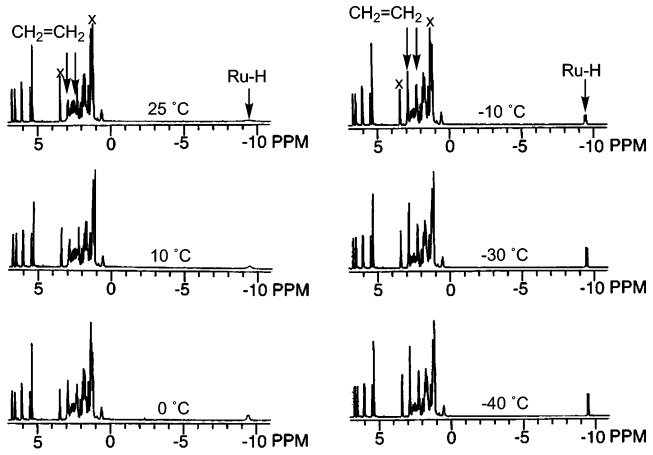

Figure 2. Variable-temperature ^{1}H NMR spectrum of [(η^6-$C_6H_5CH_2CH_2PCy_2$)RuH(CH_2=CH_2)][PF_6], **1**, in CD_2Cl_2. The symbol (×) denotes residual diethyl ether resonances.

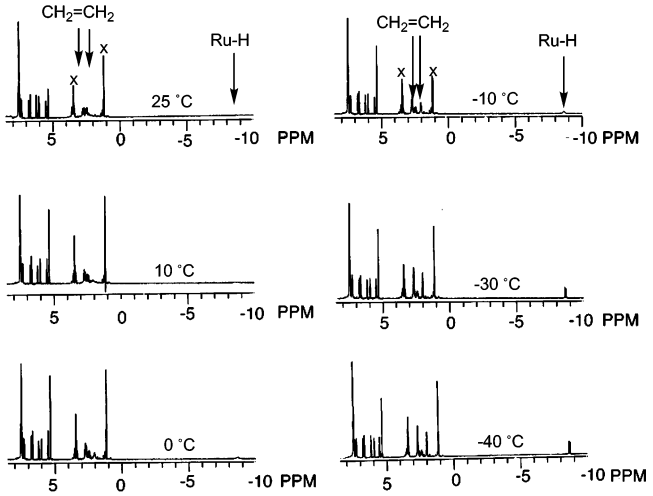

Figure 3. Variable-temperature ^{1}H NMR spectrum of [(η^6-$C_6H_5CH_2CH_2PPh_2$)RuH(CH_2=CH_2)][PF_6], **2**, in CD_2Cl_2. The symbol (×) denotes residual diethyl ether resonances.

^{1}H COSY measurements of complex **1** demonstrated that the extended multiplet over the range δ 2.34−2.71 can be assigned to the two-carbon bridge of the chelating ligand, and the resonances at δ 2.35 and 2.89 can be assigned to the coordinated ethylene ligand. Similarly, variable-temperature ^{1}H NMR measurements of complex **2** showed that the resonances at δ 2.43 and 3.52 can be assigned to the two-carbon bridge, and the resonances at δ 2.10 and 2.70 can be assigned to the ethylene ligand. The coordinated arene ligands of complexes **1** and **2** exhibit five resonances having equivalent intensities at δ 6.7 (d), 6.5 (t), 6.1 (t), 6.0 (d), and 5.4 (t) for complex **1** and at δ 6.8 (d), 6.7 (t), 6.2 (t), 6.0 (d), and 5.5 (t) for complex **2**. In the ^{13}C NMR spectra of **1** and **2**, the resonances at δ 35.89 and 35.39, respectively, can be assigned to the carbon atoms of the coordinated ethylene ligands.[17,50]

The variable-temperature ^{1}H NMR spectra of complexes **1** and **2** are shown in Figures 2 and 3, respectively. Upon cooling to −30 °C, the broad Ru−H resonances become sharp doublets (J_{HP} = 29.1 Hz for **1** and 25.2 Hz for **2**). The large coupling constant suggests that the hydride ligands exist as terminal hydrides

(50) Kletzin, H.; Werner, H. *J. Organomet. Chem.* **1985**, *291*, 213.

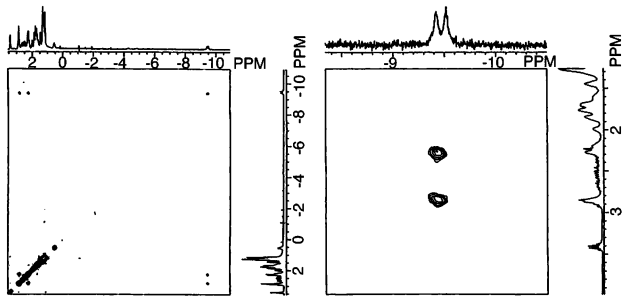

Figure 4. 2D EXSY plot of [(η^6-$C_6H_5CH_2CH_2PCy_2$)RuH(CH_2=CH_2)][PF_6], **1**, in CD_2Cl_2 at −10 °C.

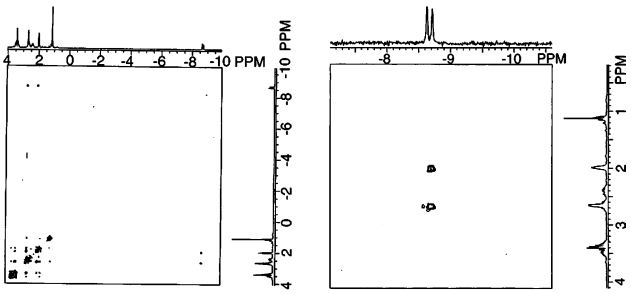

Figure 5. 2D EXSY plot of [(η^6-$C_6H_5CH_2CH_2PPh_2$)RuH(CH_2=CH_2)][PF_6], **2**, in CD_2Cl_2 at −30 °C.

rather than agostic species at this temperature.[9] In addition, cooling leads to a sharpening of the ethylene resonances. By analogy to previous studies of related metal hydride olefin complexes,[7,9,11−13] we propose that the hydride resonances are broad at room temperature due to reversible olefin−hydride insertion, as illustrated in eq 3.

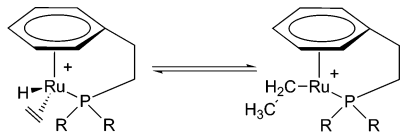

(3)

1: R = Cy
2: R = Ph

To test this hypothesis, we performed at −10 °C (for complex **1**) and at −30 °C (for complex **2**) 2D EXSY experiments, which can be used to evaluate intramolecular chemical exchange.[51] The delay time (2 s) and mixing time (1 s) used in these experiments were the same for both complexes. Upon collection of the data, correlations between Ru−H and the coordinated ethylene ligands were observed (see Figures 4 and 5). Since the cross signals possess the same phase as the diagonal signals, the cross signals cannot be assigned as NOESY signals.[52] Instead, the data provide direct evidence of olefin−hydride exchange (i.e., olefin−hydride insertion as in eq 3) within the complexes.[51]

In each of the 2D EXSY spectra shown in Figures 4 and 5, the cross-peaks between the hydride resonances and both olefinic CH_2 resonances suggest that olefin−hydride exchange occurs at both ends of the olefin. Consequently, we propose that the exchange pathway involves olefin rotation in combination with insertion/β-hydride elimination,[53] giving rise to exchange of the hydride with all four ethylene hydrogens. We note, however, that facile olefin rotation/hydride exchange was selectively inhibited in a related system investigated by Faller and co-workers, [(*p*-cymene)RuH(CH_2=CHPh)PR_3]$^+$, where exchange was observed between the hydride and only the terminal olefinic hydrogens.[11] While the presence of the relatively bulky phenyl ring in the latter system can plausibly block the pathway to exchange of the remaining internal olefinic hydrogen, electronic effects arising from the presence of the phenyl moiety might also contribute to the distinct reactivity of the Faller complexes compared to that of **1** and **2**.

Support for olefin rotation in complexes **1** and **2** is provided by their ^{1}H NMR spectra (see Figures 2−5), which exhibit two olefinic resonances rather than four. Moreover, the two olefinic resonances showed no evidence of broadening or splitting upon cooling to temperatures as low as −60 °C (not shown), suggesting facile olefin rotation with no detectable rotation barrier. In contrast, a distinct barrier to olefin rotation was observed in the Faller system at −50 °C (as indicated by a broadening of the olefinic resonances upon cooling to −50 °C and then a re-sharpening of these resonances upon further cooling to −90 °C).[11] It is plausible that enhanced steric interactions (vide supra) and/or enhanced π-back-bonding (consistent with a longer C−C bond distance of 1.40 Å for Faller's R = Ph complex vs 1.37 Å for complex **1**) might be responsible for inhibiting olefin rotation in the Faller system.

As described in the Introduction, the direct observation of olefin−hydride insertion in ruthenium hydride olefin complexes is extremely rare,[54,55] with only two previous documented examples.[11,12] It is interesting to note that the barrier to olefin−hydride insertion is apparently lower in **1** and **2** than in the nontethered analogues [(η^6-C_6Me_6)RuH(CH_2=CH_2)PR_3][PF_6], where migratory insertion apparently fails to occur.[15,17,56] It is possible that electronic and/or steric effects imposed by the two-carbon bridge play an important role in promoting the olefin−hydride insertion observed for **1** and **2**.[57] In particular, the tethered analogues might undergo insertion due to diminished π-back-bonding, which is consistent with their shorter C−C bond distance (e.g., 1.41 Å for [(η^6-C_6Me_6)RuH(CH_2=CH_2)PPh_3]-[PF_6] vs 1.37 Å for complex **1**).[15,17]

On the basis of these results, we believe that the migratory insertion chemistry for related Ru-based

(51) Perrin, C.; Dwyer, T. *Chem. Rev.* **1990**, *90*, 935.
(52) Braun, S.; Kalinowski, H.-O.; Berger, S. *150 and More Basic NMR Experiments, A Practical Course*; Wiley-VCH: New York, 1998.
(53) For a recent Ni-based example of this process, see: Leatherman, M. D.; Svejda, S. A.; Johnson, L. K.; Brookhart, M. *J. Am. Chem. Soc.* **2003**, *125*, 3068.
(54) Ruthenium hydride olefin complexes are themselves quite rare. A search of the Cambridge X-Ray Crystallographic Database revealed only five mononuclear ruthenium hydride olefin complexes.[11,15−17,55] All complexes except for that in ref 11 exhibited well-separated hydride resonances at characteristic chemical shifts (δ −9 to −11) in their ^{1}H NMR spectra.
(55) Burn, M. J.; Frickes, M. G.; Hollander, F. J.; Bergman, R. G. *Organometallics* **1995**, *14*, 137.
(56) Although Werner observed no evidence of olefin−hydride insertion,[15,17] we cannot fully exclude this pathway for the nontethered analogues.
(57) Reactivity differences for ansa vs non-ansa systems are well known (e.g., refs 35 and 36). For recent studies of related niobium and tantulum olefin hydride complexes, see: Chirik, P. J.; Zubris, D. L.; Ackerman, L. J.; Henling, L. M.; Day, M. W.; Bercaw, J. E. *Organometallics* **2003**, *22*, 172. And: Ackerman, L. J.; Green, M. L. H.; Green, J. C.; Bercaw, J. E. *Organometallics* **2003**, *22*, 188.

complexes can perhaps be tuned by appropriate modification of the ligand system utilized in the work reported here. In particular, it might be possible to prepare a modified ligand system that offers control over β-hydride elimination, which could lead to new ruthenium-based olefin polymerization catalysts.

Conclusions

The reaction of $(\eta^6\text{-}C_6H_5CH_2CH_2PR_2)Ru(CH_3)_2$ with Ph_3CPF_6 in CH_2Cl_2 produced the cationic Ru(II) complexes $[(\eta^6\text{-}C_6H_5CH_2CH_2PR_2)RuH(CH_2{=}CH_2)][PF_6]$, where R = Cy and Ph. The cationic complexes underwent reversible olefin−hydride insertion, which was directly observed by 2D EXSY magnetic resonance experiments. The observation of this relatively rare reaction should lend new insight toward the development of ruthenium-based olefin polymerization catalysts.

Experimental Section

Materials and Methods. All solvents were dried by passage through alumina and degassed by freeze−pump−thaw methods prior to use. The compounds $(\eta^6\text{-}C_6H_5CH_2CH_2PCy_2)Ru(CH_3)_2$ and $(\eta^6\text{-}C_6H_5CH_2CH_2PPh_2)Ru(CH_3)_2$ were prepared according to literature procedures.[35,36] The compound Ph_3CPF_6 was purchased from Aldrich Chemical Co. Nuclear magnetic resonance (NMR) spectra were recorded on a General Electric QE-300 spectrometer operating at 300 MHz (for ^1H) and 75.5 MHz (for ^{13}C). Elemental analyses were performed by Oneida Research Services. The 2D EXSY experiments were performed using a published technique.[52] Specifically, three 90° pulses were applied and the delay time (2s) and mixing time (1s) were selected.

Synthesis of $[(\eta^6\text{-}C_6H_5CH_2CH_2PCy_2)RuH(CH_2{=}CH_2)][PF_6]$, 1. The starting material $(\eta^6\text{-}C_6H_5CH_2CH_2PCy_2)Ru(CH_3)_2$ (70.0 mg, 1.61×10^{-4} mol) was dissolved in 15 mL of CH_2Cl_2. To this solution was added 1.0 equiv of Ph_3CPF_6 (62.6 mg, 1.61×10^{-4} mol). The mixture was stirred for 1 h. While stirring, the color of the solution changed immediately to orange and then became light yellow. The volume of the solution was reduced to ca. 1 mL by evaporation. Diethyl ether was then added to precipitate the product, which was collected by filtration and recrystallized via slow evaporation of CH_2Cl_2. Yield of light yellow crystals of **1**: 60 mg (65%). ^1H NMR (CD_2Cl_2; 300 MHz; 273 K): δ 6.71 (d, J_{HH} = 6.9 Hz, 1 H, η^6-C_6H_5), 6.50 (t, J_{HH} = 6.9 Hz, 1 H, η^6-C_6H_5), 6.07 (t, J_{HH} = 6.9 Hz, 1 H, η^6-C_6H_5), 6.04 (d, J_{HH} = 6.9 Hz, 1 H, η^6-C_6H_5), 5.40 (t, J_{HH} = 6.9 Hz, 1 H, η^6-C_6H_5), 2.50−2.71 (m, 4 H, $C_6H_5CH_2CH_2P$), 2.89 (m, 2 H, $CH_2{=}CH_2$), 2.35 (m, 2 H, $CH_2{=}CH_2$), 1.31−2.21 (m, 22 H, Cy_2), −9.5 (br s, 1 H, Ru*H*). ^{13}C NMR (CD_2Cl_2; 75.5 MHz; 293 K): δ 122.86 (d, J_{CP} = 6.4 Hz), 101.87, 96.78, 94.78 (d, J_{CP} = 6.6 Hz), 92.24 (d, J_{CP} = 4.4 Hz), 90.72, 38.23 (d, J_{CP} = 28.3 Hz), 35.89 ($CH_2{=}CH_2$), 35.26 (d, J_{CP} = 30.6 Hz), 33.42 (d, J_{CP} = 22.3 Hz), 31.43, 29.28, 28.49, 27.93, 27.76, 27.58, 27.47, 26.30−27.20 (m). Anal. Calcd for $C_{22}H_{36}RuP_2F_6$: C, 45.75; H, 6.24. Found: C, 45.30; H, 6.10.

Synthesis of $[(\eta^6\text{-}C_6H_5CH_2CH_2PPh_2)RuH(CH_2{=}CH_2)][PF_6]$, 2. Compound **2** was prepared by dissolving $(\eta^6\text{-}C_6H_5CH_2CH_2PPh_2)Ru(CH_3)_2$ (80.0 mg, 1.90×10^{-4} mol) in 15 mL of CH_2Cl_2. To this solution was added 1.0 equiv of Ph_3CPF_6 (73.7 mg, 1.90×10^{-4} mol). As the mixture was stirred for 1 h, the color of the solution changed immediately to orange and then became light yellow. After the volume of solution was reduced to ca. 1 mL by evaporation, diethyl ether was added to precipitate a tan-colored powder, which was collected by filtration. Washing the tan-colored powder with THF afforded a light yellow powder, which again became tan-colored upon drying under vacuum. Yield of **2**: 75 mg (70%). ^1H NMR (CD_2Cl_2; 300 MHz; 273 K): δ 7.48 (m, 8 H, PPh_2), 7.35 (m, 2 H, PPh_2), 6.77 (d, J_{HH} = 6.0 Hz, 1 H, η^6-C_6H_5), 6.66 (t, J_{HH} = 6.0 Hz, 1 H, η^6-C_6H_5), 6.22 (t, J_{HH} = 6.0 Hz, 1 H, η^6-C_6H_5), 6.01 (d, J_{HH} = 6.0 Hz, 1 H, η^6-C_6H_5), 5.50 (t, J_{HH} = 6.0 Hz, 1 H, η^6-C_6H_5), 3.52 (m, 2 H, $C_6H_5CH_2CH_2P$), 2.70 (m, 2 H, $CH_2{=}CH_2$), 2.70 (m, 2 H, $C_6H_5CH_2CH_2P$), 2.10 (m, 2 H, $CH_2{=}CH_2$), −8.6 (br s, 1 H, Ru*H*). ^{13}C NMR (CD_2Cl_2; 75.5 MHz; 293 K): δ 129.5−133.0 (m), 124.30, 102.09, 95.96, 94.70, 91.74 (d, J_{CP} = 7.6 Hz), 90.80, 49.33 (d, J_{CP} = 35.5 Hz), 35.39 ($CH_2{=}CH_2$), 28.47. Due to facile decomposition, a satisfactory analysis was not obtained. Anal. Calcd for $C_{22}H_{24}RuP_2F_6$: C, 46.70; H, 4.25. Found: C, 45.79; H, 3.68.

X-ray Crystal Structure Determination. All data were collected using a Siemens SMART platform diffractometer equipped with a 1K CCD area detector. A hemisphere of data (1271 frames at 5 cm detector distance) was collected using a narrow-frame method with scan widths of 0.30° in omega and an exposure time of 30 s/frame. The first 50 frames were remeasured at the end of data collection to monitor instrument and crystal stability, and the maximum correction on I was < 1%. The data were integrated using the Siemens SAINT program with the intensities corrected for Lorentz factor, polarization, air absorption, and absorption due to variation in the path length through the detector face plate. A psi scan absorption correction was applied based on the entire data set. Redundant reflections were averaged. Final cell constants were refined using 7647 reflections having $I > 10\sigma(I)$, and these, along with other information pertinent to data collection and refinement, are listed in Table 2.

Table 2. Crystal Data and Structure Refinement for 1

empirical formula	$C_{22}H_{36}F_6P_2Ru$
fw	577.52
temperature	223(2) K
wavelength	0.71073 Å
cryst syst	monoclinic
space group	I 2/a
unit cell dimen	a = 18.5840(6) Å, α = 90° b = 7.9942(3) Å, β = 101.994(1)° c = 32.5174(10) Å, γ = 90°
volume	4725.5(3) Å^3
Z	8
density(calcd)	1.624 g/mL
abs coeff	0.854 mm^{-1}
F(000)	2368
cryst size	0.28 × 0.20 × 0.10 mm
θ range for data collection	1.28−23.50°
limiting indices	$-20 < h < 20$, $0 < k < 8$, $0 < l < 36$
no. of reflns collected	10 940
no. of indep reflns	3780 (R_{int} = 0.0243)
abs corr	empirical
max. and min. transmn	0.8349 and 0.7207
refinement method	full-matrix least-squares on F^2
data/restraints/parameters	3493/0/297
goodness-of-fit on F^2	1.390
final R indices [$I > 4\sigma(I)$]	R1 = 0.0284, wR2 = 0.0524
R indices (all data)	R1 = 0.0284, wR2 = 0.0749
largest diff peak and hole	0.438 and −0.343

Acknowledgment. The Robert A. Welch Foundation (Grant E-1320) and the National Science Foundation (CAREER Award to T.R.L. CHE-9625003) provided generous support for this research. We thank Dr. Charles Anderson for experimental design and technical assistance with the NMR studies. We also thank Dr. James Korp for assistance with the X-ray crystallographic data collection and analysis.

Supporting Information Available: CIF data for complex **1**. This material is available free of charge via the Internet at http://pubs.acs.org.

OM0301987